SIMULATION OF A STIRLING ENGINE USED FOR A MICRO SOLAR POWER PLANT: 0-D MODELLING, COMPARISON WITH 1-D MODELLING

Nadia Martaj[1*], Lavinia Grosu[2], Pierre Rochelle[2], Antoine Mathieu[2], Michel Feidt[3]

[1]EPF-Ecole d'Ingénieurs, 21 boulevard Berthelot, 34000 Montpellier

[2]Laboratoire Energétique, Mécanique et Electromagnétisme, Université Paris Ouest, 50 rue de Sèvres, 92410 Ville d'Avray

[3]Laboratoire Energétique et Mécanique Théorique et Appliquée, Université Henri Poincaré, 2 avenue de la Forêt de Haye, 54000 Vandoeuvre Lès Nancy

Abstract

The goal of this paper is to determine the characteristics of a Stirling engine able to be used by a micro-solar power plant as energy conversion system. The purpose is to use solar energy as heat source and a Stirling engine because of its numerous advantages, as its high (theoretical) efficiency. This work was made in collaboration with several industrials involved in the project named MiCST, whom objective is to electrify remote villages in Africa. Results of a simple 0-D model built on Matlab®/Simulink® environment to predict engine behavior are compared with those of several 1-D models which take into account several energy losses. It is shown that 0-D model over-estimates the power but keeps its interest because of its simplicity, easy adaptability into a global model of a more complex system and reduced computing time. Empirical correlations whose coefficients are obtained according to experimental results may be used to estimate directly the total power loss.

Keywords: energy balance, energy losses, Stirling engine, solar power plant, thermodynamic model

1. Introduction

Using solar energy to operate Stirling engines with high thermal efficiency is an idea which was considered by many authors, because of the easy adaptability of the Stirling engine on low and moderate temperature sources (recovery or renewable sources). (Howell and Bannerot, 1977; Mathieu et al., 2010; Nepveu et al., 2009; Zhai et al., 2009; Bonnet, 2005).

* Author to whom all correspondence should be addressed: E-mail: nadia.martaj@epf.fr

In this study, results concerning an industrial project of an autonomous micro solar power plant (MiCST) are presented. The choice of simple and robust elements to produce electricity for remote sites in emerging countries is the main constraint of the project. The use of ecological fluids is also required, in order to have little impact on the environment.

The solar power plant should provide about 50 kWh/day. A thermal storage should be used to respond on the night request in electricity (one night of autonomy is considered for sizing the solar field).

Solar field could be realized with moderate-temperature linear concentrators. The heat storage could be achieved by sensible heat at moderate temperature (<200°C) using materials which will be locally available (sand, clay, etc.) or simply pressurized water.

A total electrical power about 10kW will be produced by several Stirling engines in parallel. This engine is chosen because of its very limited environmental impact and its high efficiency (Stouffs et al., 2002; Chen et al., 2007; Cinar et al., 2007; Martaj, 2008; Grosu and Rochelle, 2009; Karabulut et al., 2013; Aksoy et al., 2013; Solmaz et al, 2014).

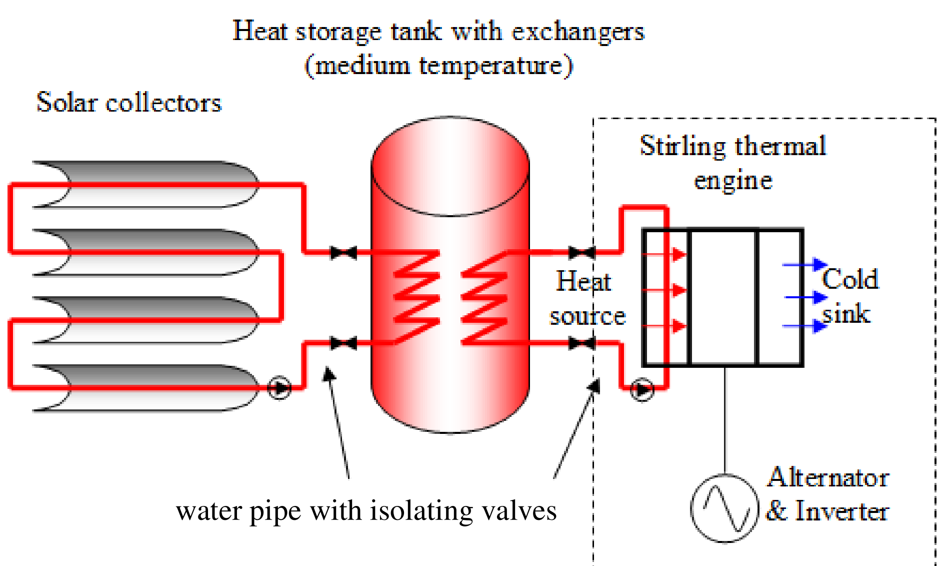

Fig. 1. Schematic diagram of the micro solar power plant

In order to develop a simulation program of the micro solar power plant (Fig.1), which will be used to control the energy commands and parameters, a simple Simulink model of the Stirling engine was defined. This model represents an integrated part in the global model of the whole system.

The Stirling engine model is a zero-dimensional adiabatic analysis, with uniform instantaneous gas pressure, based on the laws of thermodynamics. First of all, the Alpha type Stirling engine was divided in 5 volumes connected each-other (Fig.2):

- expansion space (e),
- hot exchanger (h),
- regenerator (r),
- cold exchanger (k),
- compression space (c).

The expansion and compression spaces are adiabatic volumes which vary according to the pistons motions. Heat exchange is concentrated on the three exchangers (cold, hot and regenerator spaces) whose volumes are constant.

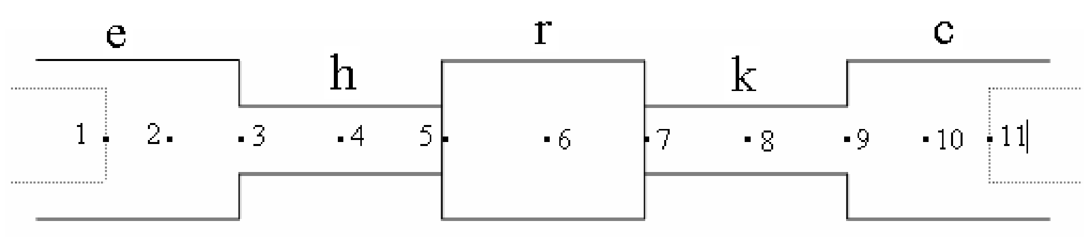

Fig. 2. Standard Alpha Stirling engine divided in 5 volumes

Points from 1 to 11 are placed on the Stirling engine scheme (Fig. 2), on the middle and the extremities on each space. The direction of mass flow is considered positive in accordance with the ascending sequence of the volume index (from left to right).

2. Characteristics of the Stirling engine

The main geometrical dimensions of the engine were defined taking into account industrial partners' considerations (MiCST project) and are given in Fig.3 and Table1.

Table 1. Geometrical characteristics of the engine

Engine dimensions	Value	Unit	Calculated parameters	Expression	Unit
$e_h=e_k=e_r$	$5*10^{-4}$	m	S_h	$Np.e_h.l_h$	m^2
$R_e=R_c$	0.1	m	S_r	$Np.e_r.l_r$	m^2
$C_e=C_c$	0.1	m	S_k	$Np.e_k.l_k$	m^2
φ_0	$\pi/2$	rad	S_e	πR_e^2	m^2
Np	67	-	S_c	πR_c^2	m^2
$l_h=l_r=l_k$	0.2	m	A_h	$2.Np.l_h L_h$	m^2
$L_k=L_k$	0.2	m	A_r	$2.Np.l_r L_r$	m^2
L_r	0.5	m	A_k	$2.Np.l_k L_k$	m^2
H_m	$2*10^{-3}$	m	V_e	$\pi R_e^2(C_e+H_m)$	m^3
			V_c	$\pi R_c^2(C_c+H_m)$	m^3
			D_h	$2\ e_h$	m
			D_r	$2\ e_r$	m
			D_k	$2\ e_k$	m

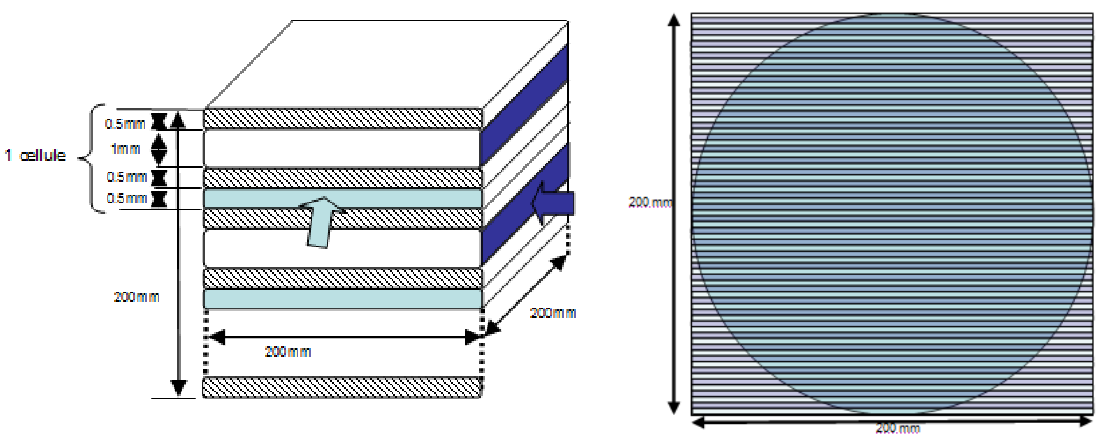

Fig. 3. Hot and cold heat exchangers geometry

The thermodynamic parameters of the studied engine are presented in Table 2.

Table 2. Thermodynamic data of the engine

Thermodynamic parameters	**Value**	**Unit**
T_{wh}	533	°K
T_{wk}	333	°K
c_p	1004	$J.kg^{-1}.K^{-1}$
r	287	$J.kg^{-1}.K^{-1}$
$k_h=k_k$	900	$W.m^{-2}K^{-1}$

The calculation of heat flows and mechanical power for a chosen, constant angular speed requires the implicit knowledge of an initial state, in terms of expansion and compression spaces volumes, as well as working gas pressure and temperature. The initial crank-angle, that defines initial volumes, has been chosen so that the initial gas velocity is close to zero.

Table 3. Initial conditions of the thermodynamic model

Parameters	**Values**	**Unit**
p_i	2000000	Pa
φ_i	$\pi * 187/180$	°
V_{e_i}	$\pi R_e^2 \left(\frac{C_e}{2}(1-\cos\varphi_i) + H_m \right)$	m^3
V_{c_i}	$\pi R_c^2 \left(\frac{C_c}{2}(1-\cos(\varphi_i-\varphi_0) + H_m \right)$	m^3

3. Description of the model

This analysis concerns the division of the engine in five elementary spaces: two adiabatic volumes (expansion and compression spaces), two isothermal heat-exchangers (hot and cold exchangers) and a regenerator whose output temperature depends on the regeneration efficiency. Working gas is assumed an ideal gas. To evaluate the mass of the fluid in each volume, ideal gas law is applied into the 5 spaces of the engine:

$$m_c = \frac{pV_c}{rT_{10}} \qquad m_k = \frac{pV_k}{rT_8} \qquad m_r = \frac{pV_r}{rT_6} \qquad m_h = \frac{pV_h}{rT_4} \qquad m_e = \frac{pV_e}{rT_2} \qquad (1)$$

Total mass of the working gas, m is the sum of the five masses above (1). Thus, instantaneous pressure, assumed uniform in the engine, is obtained using the following equation:

$$p = mr \Big/ \left(\frac{V_e}{T_e} + \frac{V_h}{T_h} + \frac{V_r}{T_r} + \frac{V_k}{T_k} + \frac{V_c}{T_c} \right) \tag{2}$$

The volumes of hot exchanger (V_h), cold exchanger (V_k) and regenerator (V_r) represent the product of their length by their frontal area (Fig.3):

$$V_h = L_h S_h \text{ , } V_r = L_r S_r \text{ and } V_k = L_k S_k \tag{3}$$

The instantaneous volumes of expansion space (V_e) and compression space (V_c) are given according to the geometrical dimensions of the cylinders and the pistons motion – instantaneous position of the pistons.

$$V_e = \frac{C_e}{2}\left(1 - \cos(\omega t + \varphi_i)\right) S_e + H_m S_e \tag{4}$$

$$V_c = \frac{C_c}{2}\left(1 - \cos(\omega t + \varphi_i - \varphi_0)\right) S_c + H_m S_c \tag{5}$$

Mean temperatures T_h, T_k and T_r are considered for corresponding spaces. Temperatures of hot volume T_h and cold volume T_k, are obtained using expressions of the convective heat flows transferred to the working fluid:

$$\dot{Q}_h = k_h A_h (T_{wh} - T_h) \tag{6}$$

$$\dot{Q}_k = k_k A_k (T_k - T_{wk}) \tag{7}$$

where T_{wh} and T_{wk} are cylinders walls temperatures and k_h and k_k are heat transfer coefficients.

Thus,
$$T_h = T_{wh} - \dot{Q}_h \big/ (k_h S_h) = T_4 \tag{8}$$

$$T_k = T_{wk} + \dot{Q}_k \big/ (k_k S_k) = T_8 \tag{9}$$

Temperature evolution along the regenerator is supposed linear, thus regenerator temperature is defined as a logarithmic average of T_h and T_k.

$$T_6 = (T_4 - T_8) \Big/ ln \frac{T_4}{T_8} \tag{10}$$

The elementary mass variation in the adiabatic compression space is obtained by applying the energy balance in this space.

$$dm_c = \left(pdV_c + V_c \frac{dp}{\gamma} \right) \Big/ rT_9 \tag{11}$$

To calculate interface temperature (T_9), it is necessary to take into account the gas flow direction. Thus if $dm_c < 0$ then $T_9 = T_{10}$, else $T_9 = T_8$.

In the same way, expansion space mass variation dm_e is given by the following equation:

$$dm_e = \left(pdV_e + V_e \frac{dp}{\gamma} \right) \Big/ rT_3 \tag{12}$$

with the corresponding assumption on the interface temperature (exchanger/expansion space): if $dm_e > 0$ then $T_3 = T_2$, else $T_3 = T_4$.

Differential form of the ideal gas law is used in order to determine the elementary mass variation within the heat exchangers:

$$\begin{cases} dm_k = m_k\, dp/p = V_k/rT_k \cdot dp \\ dm_r = m_r\, dp/dp = V_r/rT_r \cdot dp \\ dm_h = m_h\, dp/p = V_h/rT_h \cdot dp \end{cases} \tag{13}$$

Moreover, the sum of the 5 elementary mass variations - or the whole engine mass variation – should be null, assuming a zero-leakage (constant internal gas mass).

$$\sum dm_j = \frac{dp}{r}\left[V_e/\gamma T_3 + V_h/T_h + V_r/T_r + V_k/T_k + V_c/\gamma T_9\right] + \frac{p}{r}\left[dV_e/T_3 + dV_c/T_9\right] = 0 \tag{14}$$

Equation (14) leads to the differential pressure expression:

$$dp = -\gamma\, p\left(\frac{dV_c}{T_9} + \frac{dV_e}{T_3}\right) \Big/ \left[\frac{V_c}{T_9} + \gamma\left(\frac{V_k}{T_8} + \frac{V_r}{T_6} + \frac{V_h}{T_4}\right) + \frac{V_e}{T_3}\right] \tag{15}$$

Combining equations (11), (12) and (13), T_{10} and T_2 could be obtained:

$$\begin{aligned} \frac{dT_{10}}{T_{10}} &= \left(1 - \frac{T_{10}}{\gamma T_9}\right)\frac{dp}{p} + \left(1 - \frac{T_{10}}{T_9}\right)\frac{dV_c}{V_c} \\ \frac{dT_2}{T_2} &= \left(1 - \frac{T_2}{\gamma T_3}\right)\frac{dp}{p} + \left(1 - \frac{T_2}{T_3}\right)\frac{dV_e}{V_e} \end{aligned} \tag{16}$$

The sign of the elementary masses transferred through the spaces interfaces depends on the gas flow direction in the engine (positive from the left to the right, see Fig.2). They are calculated using (Eq. 17).

$$\begin{cases} dm_c = dm_9 \\ dm_k = dm_7 - dm_9 \Leftrightarrow dm_7 = dm_k + dm_c \\ dm_r = dm_5 - dm_7 \Leftrightarrow dm_5 = dm_k + dm_c + dm_r \\ dm_h = dm_3 - dm_5 \Leftrightarrow dm_3 = dm_k + dm_c + dm_r + dm_h \\ dm_e = -dm_3 \end{cases} \tag{17}$$

The thermal energies exchanged on the hot/cold exchangers, and on the regenerator are obtained using energy balance applied to each of these 3 spaces.

$$\begin{cases} dQ_k = \dfrac{c_v}{r} V_k\, dp - c_p\,(T_7\, dm_7 - T_9\, dm_9) \\ dQ_r = \dfrac{c_v}{r} V_r\, dp - c_p\, (T_5 dm_5 - T_7\, dm_7) \\ dQ_h = \dfrac{c_v}{r} V_h\, dp - c_p\, (T_3\, dm_3 - T_5\, dm_5) \end{cases} \tag{18}$$

The regeneration efficiency is:

$$\eta_r \approx \frac{T_4 - \Delta T - T_8}{T_4 - T_8} \tag{19}$$

where ΔT is the gas temperature difference between the outlet of the regenerator and the hot or cold volume one ($\Delta T = T_4 - T_5 = T_7 - T_8$).

T_5 and T_7 depend on the flow direction:

if $dm_5 < 0$ then $T_5 = T_4 - \Delta T$, else $T_5 = T_4$

if $dm_7 < 0$ then $T_7 = T_8$, else $T_7 = T_8 + \Delta T$

Differential work, in the compression space dW_c and in the expansion one dW_e, can be calculated using the instantaneous pressure and the elementary variation of respectively compression and expansion volumes.

$$\begin{cases} \delta W_c = - p dV_c \\ \delta W_e = - p dV_e \end{cases} \tag{20}$$

The sum of these two previous expressions represents the elementary work provided by the engine cycle. After integration, mechanical energy provided by a complete cycle is determined.

4. Results of simulation

Fig.4 shows the indicator diagram (p, V) of the compression and expansion spaces for the 20th cycle iteration. The sum of the surfaces defined by the green-spotted intersection areas of these cycles, with the affected signs, symbolizes the work provided by cycle ($W = -\oint p dV_c - \oint p dV_e$). The pressure varies from 1.7 10^6 to 5 10^6 Pa.

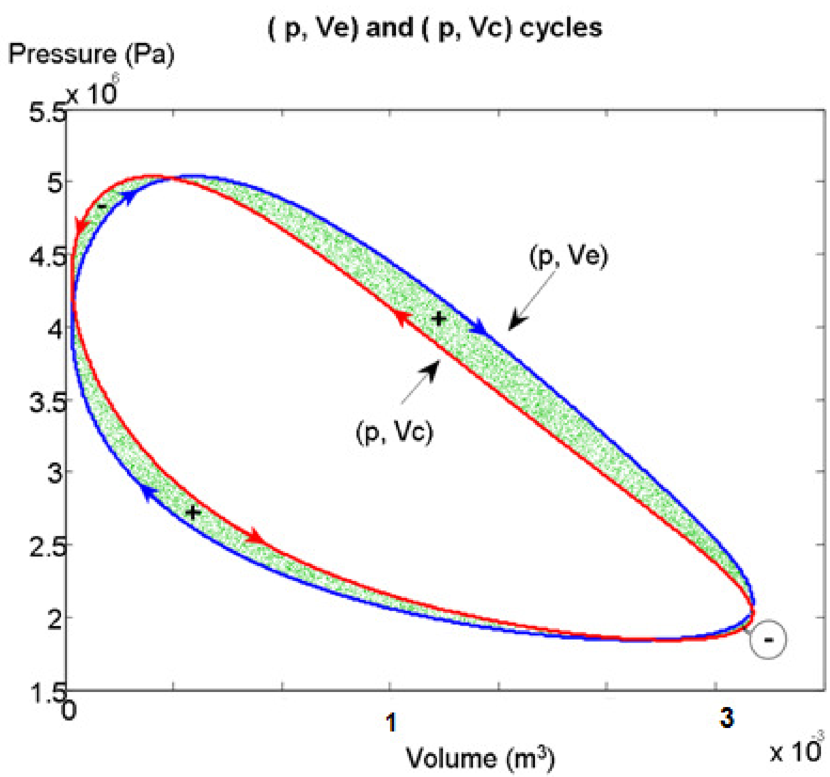

Fig. 4. Indicator diagram (p, V) of the compression and expansion spaces

Some simulation results for engine speed about 300 tr/min are shown on table 4. Indicated mechanical power supplied by the Stirling engine is about 9425W, which correspond to a heat flow rate on the hot source about 114000W. In these conditions the efficiency is very correct, around 8,27%, taken into account the low level of the hot source temperature.

Table 4. Simulation results for 300 tr/min

Parameters	**Values**
Heat received on the hot exchanger Q_h, [J/cycle]	22800
Heat difference on the regenerator, ΔQ_r, [J/cycle]	-822.1
Heat supplied on the cold exchanger Q_k, [J/cycle]	-20020
Indicated work W, [J/cycle]	-1885
Relative error in the energy balance [%]	3.8
Indicated power $\dot{W}$, [W]	-9425
Heat flow on the hot exchanger $\dot{Q}_h$ [W]	114000
Heat flow on the regenerator $\dot{Q}_r$ [W]	-4110.5
Heat flow on the cold exchanger $\dot{Q}_k$ [W]	-100100

Pressure losses and mechanical losses are not considered in this model, and convective heat transfer dependence on engine speed is neglected. The convective heat transfer coefficient is assumed to be constant, about 900 $W/m^2 K$.

The assumption on the regenerator interface temperatures implies homogeneous gas densities and mixtures. This assumption has consequences on the simulation results which move away from the real results. A solution to this problem might be an accurate consideration of the regenerator temperature gradient. Thus, it is necessary to divide the volume of the regenerator into several isothermal cells.

5. Comparison with the results of 1-D simulations

The results obtained from 0-D simulation presented on table 4, have been compared with those obtained with a second Matlab program, based on a 1-D model of the engine. Five main volumes are considered, with several equal divisions of the regenerator volume, and various rates of energy losses. Auxiliary cells are considered on the interface between two spaces, like is shown on figure 5.

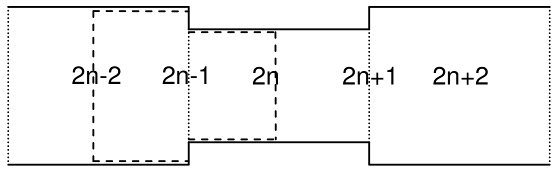

Fig 5: Scheme for 1-D Modelling with auxiliary cells on the interface

Mass balance and energy balance are applied on each space and momentum equation is applied on each auxiliary cell. Thus, gas density and velocity are defined different on each interface (2n-1, 2n+1, etc).

Table 5 and Figure 6 show the importance of each energy loss, and their influence on the total power provided by the engine. One remarks that a 0-D model widely over-estimates the power compared to the possible performance of this engine. On the other hand this model keeps its interest because of its simplicity and easy adaptability into a global model of a complex system and reduced computing time, which is an important constraint of this project. Some improvements may be achieved as using empirical correlations whose coefficients are obtained according to experimental results. These correlations could estimate the total power loss or only pressure losses (Petrescu et al., 2003).

The division of the regenerator space in several cells (volumes) is essential for a better representation of heat and mass transfer phenomena. But, an analysis of models 2, 3 and 4, leads to realize that five elementary cells allow already a good modelling of the regenerator with a limited computing time.

Pressure losses coefficient is considered constant about 0,04 or depending on Reynolds number ($f = 0{,}32\,Re^{-0{,}25}$). Exchanger's wall material is aluminium with a thickness about 0.5mm. Thermal conductivity value λ is considered linear between 273W/mK for 300K and 237 W/mK for 500K. External fluid velocity is about 5m/s and external convection is considered to be defined by the correlation: $Nu = 0{,}023\,Re^{0{,}8}\,Pr^{0{,}4}$. In these conditions, thermal inertia of heat exchanger's wall is studied (using Fourier and Newton laws) and a comparison between Model 3 and Model 5 leads to remark a diminution of mechanical power from 5334W to 4820W. In addition to this, one notes a small wall temperature fluctuation about 1°C only.

Gas leakage is estimated using following expression [Homutescu, 2008]:

$$\dot{m}_l = -\rho \frac{\pi D \delta^3}{12\mu} \frac{\Delta p}{L_d} \tag{21}$$

with D : piston diameter, Ld : seal height, μ: gas dynamic viscosity, δ : distance seal/cylinder and, Δp : pressure difference between two faces of the piston. For the Model 6, δ is supposed about 1/100 mm and Ld=1cm. Gas leakage implies a power loss about 1534W (comparison of Model 5 with Model 6).

Table 5. Comparison of power values obtained by 0-D and 1-D models

	Description	Power [W]
Model 1	0-D model	-9425
Model 2	1-D model - 5 volumes and 5 cells in the regenerator - pressure losses, f=0.04	-5610
Model 3	1-D model - 5 volumes and 10 cells in the regenerator - pressure losses, f=f(Re)	-5334
Model 4	1-D model 5 volumes and 20 cells in the regenerator - pressure losses, f=f(Re)	-5488
Model 5	1-D model - 5 volumes and 10 cells in the regenerator - pressure losses, f=f(Re) - thermal inertia of walls made of 0.5 mm thick Aluminium	-4820
Model 6	1-D model - 5 volumes and 10 cells in the regenerator - pressure losses f=f(Re) - thermal inertia of walls made of 0.5 mm thick Aluminium, - gas leakage.	-3286

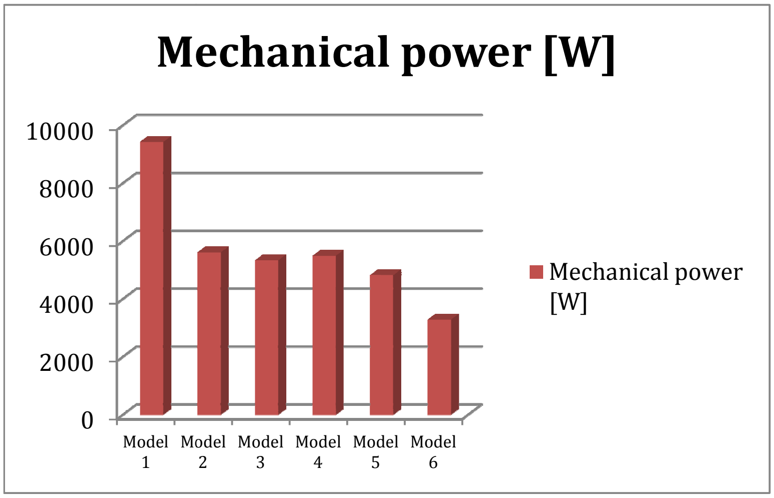

Fig 6: Simulation results for six different models

6. Conclusion

In this paper, results concerning an industrial project of an autonomous micro solar power plant (MiCST) are presented. The choice of simple and robust elements to produce electricity for remote sites in emerging countries is the main constraint of the project. The use of ecological fluids is also required, in order to have little impact on the environment.

In order to develop a simulation program of the micro solar power plant, which will be used to control the energy commands and parameters, a simple Simulink model of the Stirling engine was defined. This model represents a part integrated in the global model of the whole system.

A Stirling engine is studied using a 0-D model, namely adiabatic model because of the adiabaticity supposed on the compression and expansion spaces. The engine is divided on five spaces; ideal working gas and instantaneous uniform gas pressure are the principal assumptions of the model based on the thermodynamics laws and the kinematics motion of the pistons.

This model leads to predict the engine behaviour for several operating point. The results are compared with those obtained with several 1-D models, that take into account various energy losses.

It is shown that 0-D model over-estimates the power but keeps its interest because of its simplicity, easy adaptability into a global model of a complex system and reduced computing time. Empirical correlations whose coefficients are obtained according to experimental results may be used to estimate directly the total power losses.

Nomenclature

A	exchanger heat transfer area [m^2]
c_p	specific heat at constant pressure, [$J.kg^{-1}\ K^{-1}$]
C	piston stroke, [m]
D	hydraulic diameter, [m]
e	inter-plate distance, [m]
f	coefficient of pressure losses, [-]
H	height, [m]
k	convective heat transfer coefficient, [$W.m^{-2}.K^{-1}$]
l	exchanger width, [m]
L	exchanger length, [m]
m	mass, [kg]
N	engine speed, [rpm]
Np	number of passages through the exchangers, [-]
p	pressure, [Pa]
$\dot{Q}$	heat flow, [W]
Q	heat, [J/cycle]
r	gas constant , [$J.kg^{-1}\ K^{-1}$]
R	piston radius, [m]
S	gas frontal free-flow area [m^2]
T	temperature, [K]
t	time, [s]
V	volume, [m^3]
W	work, [J/cycle]
$\dot{W}$	mechanical power, [W]

Greek Letters

φ	rotation angle, [°]
φ_0	phase shift between the pistons, [°]
ω	angular speed, [rad/s]

Indices

c compression

e expansion

h hot

i initial

k cold

m dead volume

p operating piston

r regenerator

w wall

Acknowledgements

The authors gratefully acknowledge Schneider Electric - leader of MiCST project - and all the partners of the consortium: Barriquand Technologies Thermiques, CEA-INES, Cedrat Technologies, Défi Systèmes, Exosun, LEME, LEMTA, Mecachrome France, SAED and Stiral. The authors also gratefully acknowledge the ADEME, which finances the MiCST project.

References

Aksoy F., Cinar C. (2013). Thermodynamic analysis of a beta-type Stirling engine with rhombic drive mechanism. Energy Conversion and Management, 75(319-324).

Andersen S.K., Carlsen H., Per Grove Thomsen, (2005), Preliminary results from simulations of temperature oscillations in Stirling engine regenerator matrices, Energy, p. 1–13.

Bonnet, S., (2005), Moteurs Thermiques À Apport de Chaleur Externe: Étude d'un Moteur Stirling et d'un Moteur Ericsson. PhD thesis, Université de Pau et des Pays de l'Adour.

Chen L., Zhan W., Sun F., (2007), Power, efficiency, entropy-generation rate and ecological optimization for a class of generalized irreversible universal heat-engine cycles, Applied Energy 84, p. 512-525.

Cinar C. (2007). Thermodynamic Analysis of an α;-Type Stirling Engine with Variable Phase Angle. Journal of Mechanical Engineering Science, 221(949-954).

Ercan Ataer, Karabulut H., (2005), Thermodynamic analysis of the V-type Stirling-cycle refrigerator, International Journal of Refrigeration 28, p. 183–189.

Finkelstein T. (1961) Generalized thermodynamic analysis of Stirling engines (paper 118B) and Optimization of phase angle and volume ratios in Stirling engines (paper 118C), SAE Annual Winter Meeting, Detroit, USA.

Grosu, L., Rochelle, P., (2009), Application de la méthode de Schmidt avec régénération imparfaite aux 3 types de moteur Stirling. Nouvelles solutions analytiques, congrès SFT, Vol.2, p. 895-901, Vannes, France.

Homutescu V. M., Dumitraşcu G., Horbaniuc B., (2008), Evaluation of the work lost due to leaks through cylinder-displacer GAP, COFRET'08, Nantes.

Howell J., Bannerot R., (1977), Optimum solar collector operation for maximizing cycle work output. University of Houston. Solar Energy 19, p. 149-15.

Karabulut H., Solmaz H., Okur M., Şahin F. (2013). Dynamic and Thermodynamic Analysis of Gamma Type Free-Piston Stirling Engine. Journal Of The Faculty Of Engineering and Architecture of Gazi University, 28(265-273).

Martaj N., (2008), Modélisation Energétique et exergétique, simulation et optimisation des moteurs Stirling à faible différence de température – Confrontation avec l'expérience, Thèse de doctorat, Université Paris Ouest Nanterre la Défense, Paris, France.

Mathieu, A., Feidt, M., Rochelle, P., Grosu, L., Gualino, D., Grappe, B., (2010), Preliminary sizing and optimization of a micro solar power plant by a parametric sensitivity study, Environmental Engineering and Management Journal, Vol. 9, No. 10, p. 1361-1387.

Nepveu, F. et al., (2009), Thermal model of dish/Stirling systems, Solar Energy, Vol. 83, p. 81–89.

Organ A.J., (1997), The Regenerator and the Stirling Engine, Wiley ed., ISBN 1860658010-6.

Parlak N., Wagner A., Elsner M., Soyhan H.S., (2009), Thermodynamic analysis of a Gamma type Stirling engine in non-ideal adiabatic conditions, Renewable Energy 34, 266-273.

Petrescu S. et al., (2003), Application of the Direct Method to Irreversible Stirling Cycles with Finite Speed, Int. J. of Energy Research, 26, p. 589-609.

Rochelle P. and Grosu L., (2011) Analytical solutions and optimization of the exoirreversible Schmidt cycle with imperfect regeneration for the 3 classical types of Stirling engine, Oil&Gas Science and Technology, Vol. 66, N° 5, pp. 747-758.

Senft J.R.(1998), Theoretical limits on the performance of Stirling engines, Int. J. Energy Res. 22, p. 991-1000.

Solmaz H., Karabulut H. (2014). Performance Comparison of a Novel Configuration of Beta-type Stirling Engines With Rhombic Drive Engine. Energy Conversion and Management, 78(627–633).

Stouffs, P., Bonnet, S., Alaphilippe, M., (2002), Etude expérimentale des transferts thermiques et des transformations thermodynamiques dans un petit moteur Stirling, Elsevier, proceeding SFT, p. 763-768.

Tlili I., Timoumi Y., Ben Nasrallah S., (2007), Thermodynamic analysis of Stirling heat engine with regenerative losses and internal irreversibilities, Int. J. Engine Res. Vol.9, p. 45-56.

Wang J.T., Chen J., (2002), Influence of several irreversible losses on the performance of a ferroelectric Stirling refrigeration-cycle, Applied energy 72, p. 495–511.

Wu F., Chen L., Wu C., Sun F., (1998), Optimum performance of irreversible Stirling engine with imperfect regeneration, Energy Conversion Management Vol. 39, No. 8, p. 727-732.

Zhai H., Dai Y.J., Wu J.Y., Wang R.Z., (2009), Energy and exergy analyses on a novel hybrid solar heating, cooling and power generation system for remote areas, Applied Energy, Volume 86, Issue 9, p. 1395-1404.